FORMATION OF ICE-RICH LOBATE DEBRIS APRONS THROUGH REGIONAL ICESHEET COLLAPSE AND DEBRIS-COVER ARMORING. J. L. Fastook[1], J. W. Head[2], and D. R. Marchant[3]; [1]University of Maine, Orono, ME 04469, fastook@maine.edu, [2]Brown University, Providence, RI, [3]Boston University, Boston, MA.

Introduction: Models of ice sheets on Mars have helped to assess and interpret glacial deposits interpreted from orbital data [e.g., 1-2], while also testing hypothetical scenarios that may have been responsible for their formation [3-4]. In many of these cases the ice sheets themselves existed only in the past during periods of different climate dictated primarily by dramatic changes in obliquity [3, 5-6]. In this analysis we are assessing a possible formation mechanism for the lobate debris aprons (LDA) interpreted to be debris-covered glaciers [2,7] that have recently been proven to contain hundreds of meters of relatively pure water ice [8-10].

LDAs in the Deuteronilus Mensae region in the fretted terrain along the dichotomy boundary [11] have been recognized to involve significant amounts of water ice since Viking observations [12-13], but controversy over the amount of water ice involved has ranged from very low (~20-30%, ice assisted talus flow [14-15]), medium (~30-80% rock-glaciers [16], and high (>80% debris-covered glaciers [17-20]). In addition, the low number of craters on the LDA surfaces requires mid-to-late Amazonian ages for either formation, or the latest movement and deformation [21]

Recent subsurface radar sounding from orbiting spacecraft (SHARAD on MRO [22]) has confirmed that many, if not most, of the LDAs contain relatively pure water ice covered only by a thin layer of debris shed from adjacent scarps [8-10]. Their requirement that the valley floor extend undistorted beneath the observed LDAs dictated a dielectric constant consistent with pure water ice (<10% contaminant). In addition, they can constrain the surface debris layer to be less than ~10 m due to the lack of a shallow soil-ice interface in the radar data, but they point out that it must be greater than 0.5 m to explain the lack of a hydrogen signal in gamma ray/neutron data [23-25].

Figure 1 shows a radargram and ground track from [10] for a LDA at 39.1N, 24.2E in the Deuteronilus Mensae region. Focusing on the feature in the left-hand side of the track, where it crosses between two mesas one observes a profile of the figure showing a classic convex profile indicative of viscous flow. How does this surface debris cover form?

Formation Hypothesis: On the basis of our glacial flow modeling, the formation mechanism begins with a larger regional ice sheet that completely drowns the terrain [2, 5, 26-27]. As this ice sheet collapses in an ablating environment, its surface drops below the level of the scarps where current LDAs are found. At this

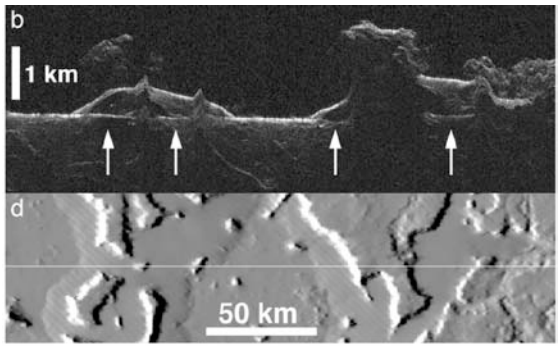

Figure 1.

point debris from the scarps begins to accumulate on the ice sheet surface. As with our terrestrial analog, the Mullins Glacier in the Dry Valleys of Antarctica [28-32], this debris cover armors the surface and reduces ablation by orders of magnitude. As the initial armoring begins at the base of the scarps, the ice sheet will begin to evolve a surface slope down away from the scarp. This surface slope will carry surface debris away from the scarp expanding the armored area. As the sheet continues its collapse, at some point the entrained debris will reach the bed surface and the entire profile is completely armored by debris, leaving behind a LDA with a particular thickness and lateral extent that depends on the choice of certain parameters within the model.

Modeling: The model is a 1D flowband shallow-ice formulation simplified by assuming isothermal conditions (specifiable uniform temperature in the flowband interior). This is reasonable given the low flow velocities and typical thicknesses of LDAs of a few hundred meters. Other parameters in the model besides temperature, which determines flow rates in the evolving LDA, include the debris-free sublimation rate, the limiting debris-covered sublimation rate, the debris accumulation rate at the base of the scarp, a factor relating the depth of debris cover to the reduction in sublimation rate, and the height of the scarp at which debris begins to accumulate.

Experiments: Extensive model runs with randomly chosen values for the various input parameters yield a suite of final configurations from which target thicknesses and lateral extents can be examined. We define a "distance" metric that is a measure of the goodness of the result to the desired target, where T_0 and M_0 are the target thickness and margin extent respectively.

$$D = \sqrt{\left(\frac{(T - T_0)}{T_0}\right)^2 + \left(\frac{(M - M_0)}{M_0}\right)^2}$$

After extensive examination of the parameter space we find that the most sensitive parameters are 1) temperature, 2) debris-free sublimation rate, and 3) scarp height. Since scarp height is reasonably well constrained by MOLA topography, we examine in detail the effects of temperature and debris-free sublimation rates. Figure 2 shows plots of margin distance and thickness as functions of temperature (°C) and debris-free sublimation rates (mm/a). One can clearly see that warmer temperatures and lower sublimation rates lead to greater margin extent, while warmer temperatures and larger sublimation rates lead to thinner LDAs.

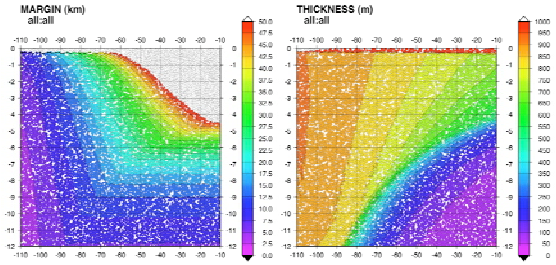

Figure 2.

Evaluation of the "distance" metric for a particular target margin extent of 20 km and thickness of 400 m yields the envelope of temperatures and sublimation rates with "distance" metric less than $10^{-0.5}$ (0.32 indicated as base-10 log) shown in Figure 3. Clearly, a best fit is obtained for a temperature of -52 C and a sublimation rate of 7.2 mm/a.

As we repeat the procedure for different target margin extents and thicknesses, we find the following behavior shown in Figure 4. Lines of constant thickness trend from lower left to upper right (200 along the lower right to 900 along the top at 50 m intervals). Lines of constant margin extent display an "L-shaped" pattern (with 10 km on the left and 40 on the upper right at 5 km intervals).

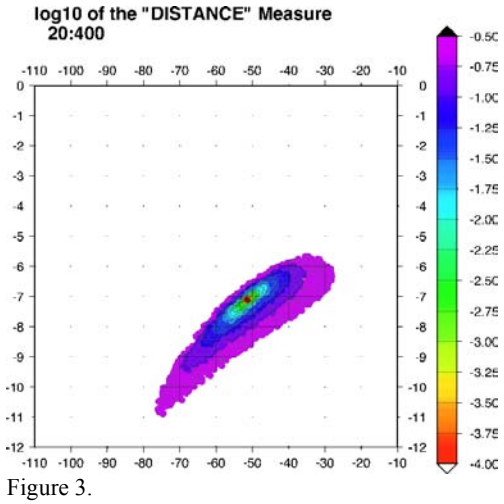

Figure 3.

Conclusions: With a simple flowband model we can set "targets" of thickness and lateral extent as more thorough mapping of LDA size and thickness is carried out. By narrowing our parameter space to temperature and debris-free sublimation, we can obtain estimates of the climate in place as the LDAs were forming during the collapse of a larger, regional ice sheet that completely drowned the local terrain [2,26].

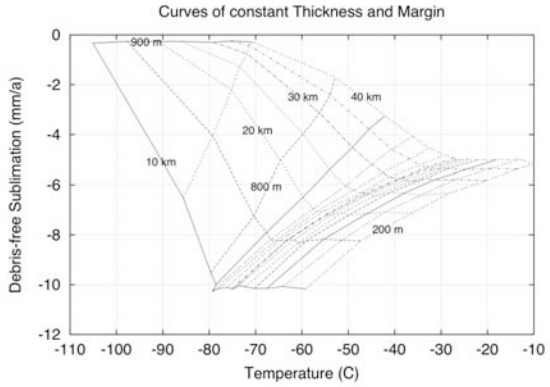

Figure 4.

References: [1] Head and Marchant (2003) *Geology 31(7)*, 641-644. [2] Head et al. (2010) *EPSL, 294*, 306-320. [3] Forget et al. (2006) *Science 5759*, 368-371. [4] Fastook et al. (2008) *Icarus 198*, 305-317. [5] Madeleine et al. (2009) *Icarus 203*, 390-405. [6] Laskar et al. (2004) *Icarus* 170, 343-364. [7] Baker et al. (2010) *Icarus* 207, 186-209. [8] Holt et al. (2008) *Science* 322 1235-1238. [9] Plaut et al. (2008) *LPS XXXIX,* Abstract #2290. [10] Plaut et al. (2009) *Geophys. Res. Lett. 36*, L02203. [11] Sharp et al. (1973) *J. Geophys. Res. 78*, 4073-4083. [12] Carr and Schaber (1977) *J. Geophys. Res. 82*, 4039-4054. [13] Lucchitta (1984) *J. Geophys. Res.*, *89*, B409–B418. [14] Squyres (1978) *Icarus*, *34*, 600-613. [15] Squyres (1979) *J. Geophys. Res. 84*, 8087-8096. [16] Mangold et al. (2002) *Planet. Space Sci. 50*, 385-401. [17] Colaprete and Jakosky (1998) *J. Geophys. Res. 103*, 5897-5909. [18] Head et al. (2005) *Nature 434*, 346-351. [19] Head et al. (2006a) *Geophys. Res. Lett. 33*, L08S03. [20] Head et al. (2006b) *Earth Planet Sci. Lett. 241*, doi:10.1016/j.epsl.2005.11.016. [21] Chuang and Crown (2005) *Icarus 179*, 24-42. [22] Seu et al. (2007) *J. Geophys. Res. 112*, E05S05. [23] Boynton et al. (2007) *J. Geophys. Res. 112*, E12S99. [24] Feldman et al. (2004) *J. Geophys. Res. 109*, E09006. [25] Mitrofanov et al. (2002) *Science 297*, 78-81. [26] Fastook et al. (2010) *LPS XLI*, Abstract #1823. [27] Fastook et al. (2010) *Icarus* in review. [28] Marchant and Head (2004) *LPS XXXV,* Abstract #1405. [29] Marchant and Head (2005) *LPS XXXVI,* Abstract #1421. [30] Marchant et al. (2007) *USGS OFR-2007*, 1-4. [31] Shean et al. (2007) *Antarctic Science 4*, 485-496. [32] Marchant et al., (2010) *LPS XLI*, Abstract #2601. [33] Kowalewski et al. (2006) *Antarctic Science* 18, 421-428.